# **Lecture 1: Evidence and Properties of Dark Matter**

Dark matter is one of the greatest open questions of 21st-century physics. It bridges fields ranging from cosmology to particle physics, and focusing too heavily on a single aspect risks giving an overly narrow view of both the evidence and the possible solutions. In just three hours, we cannot be expected to master all the details, but we will explore the most important lines of evidence, their implications for potential explanations, and the diverse approaches being pursued to detect different dark matter candidates.

Before we begin looking at the evidence I want to motivate the following sections by a historical example when data measured in gravitationally bound systems didn't line up with the theory. In the first half of the 19th century, the orbit of Uranus showed a discrepancy with the predicted orbit using Keplers laws. At times the planet seemed to speed up, at others it slowed down. The french astronomer Le Verrier and the english mathematician John Smith independently predicted an unseen mass exerting an extra gravitational pull on Uranus. Based on the data they were able to predict the orbit of this hypothetical eighth planet, which led to the discovery of the planet Neptune in 1846, see Figure 1. A problem of missing mass had been solved by identifying and discovery a body missing mass. In the meantime, data from Mercury showed some deviations as well. In the case of Mercury, it's closest approach to the sun (its perihelion) was gradually shifting, see Figure 2. This shouldn't happen in Newtonian mechanics apart from very small effects from the other planets and the sun not being perfectly spherical. Having had success with the prediction of Neptune, Le Verrier (and others) proposed another planet closer to the sun than Mercury and called in Vulcan. Even though there was some controversy this planet was never observed and instead Einsteins theory of General Relativity provided the explanation for Mercurys strange behaviour. A missing mass problem had been solved by discovering a more fundamental theory of gravity.

When should consider this a cautionary tale. When discussing the evidence for dark matter we should be careful to consider the implications

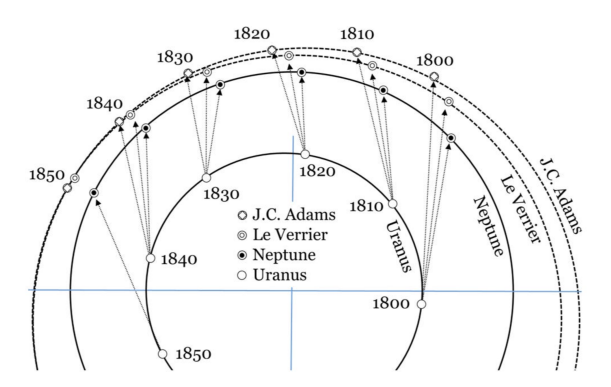


Figure 1: Trajectories of Uranus, Neptune and the projections from Le Verrier and Adams based on the anomlaous data from Uranus' orbit. Figure taken from [1].

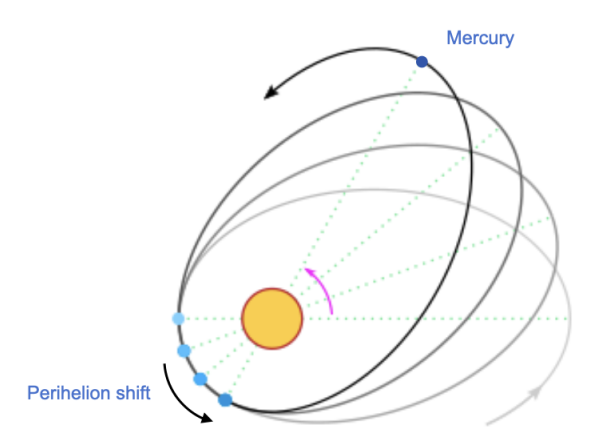


Figure 2: Precession of the perihelion of Mercury because of relativistic  $1/r^3$  corrections to the Newtonian potential. Much later, perihelion shifts were also measured for Venus, Earth and Mars for which they're much smaller. Figure adapted from [2].

#### 1.1 Galactic Rotation curves

The orbits of stars in galaxies can be modelled by a approximating the galaxy by a dense core of stars and a disk. for far out stars one can treat this as a point source at first approximation, so that the velocities of these stars should fall with the distance from the galactic centre

$$\vec{F}_G = \vec{F}_C \tag{1}$$

$$\frac{GmM}{r^2} = m\frac{v_c^2}{r} \qquad \Rightarrow \quad v_c = \sqrt{\frac{mM}{r}} \,. \tag{2}$$

Whereas this relationship is almost exactly correct for orbits in our solar system, observations from galaxies show a very different dependence. Since the first observations by the american astronomer Vera Rubin in the 1970, far from the centre the rotation curves stay constant, see Figure 3. This isn't an isolated measurement, but has been observed in thousands and thousands of galaxies. What could possibly explain that?

- A new force? Maybe gravity is different at very large distances  $r\gg R_{\rm solar\; system}$ . Maybe for very small accelerations Newtons law is modified  $\vec{F}=m\vec{a}\mu(a/a_0)$
- Maybe there is more matter? It couldn't be in a disk, but we can use the rotation curves to estimate its distribution

Starting from (1), but instead assuming an unspecified mass distribution M(r),

$$\frac{mv_c^2}{r} = \frac{GM(r)m}{r^2} \qquad \Rightarrow \qquad M(r) = \frac{v_c^2 r}{G} \,. \tag{3}$$

If  $v_c$  is constant as observed this means  $M(r) \propto r$  and the density is

$$\int d^3r \rho(r) = M(r) \qquad \Rightarrow \qquad \rho(r) = \frac{v_c^2}{4\pi G} \frac{1}{r^2} \,. \tag{4}$$

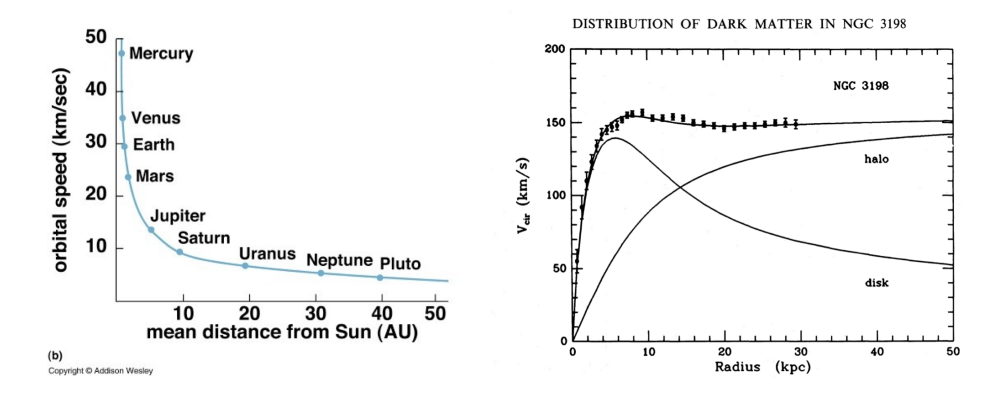


Figure 3: Left: Solar system orbits and  $v(r) \sim 1/\sqrt{r}$  law. Right: Orbits in the NGC 3198 with expected curve from a disk and a dark matter halo. Figure taken from [3].

Since the integral diverges if taken from  $r=-\infty$  to  $r=\infty$ , it needs to be cut off. As a result, a mass distributed like a spherically symmetric cloud, or *halo* in which the galaxy is embedded could explain the observations, see Figure 4. This is also what one would expect from an isothermal, self-gravitating gas  $\rho \propto 1/r^2$ . However, with just this evidence at hand we can't really decide between new law of gravity and more matter.

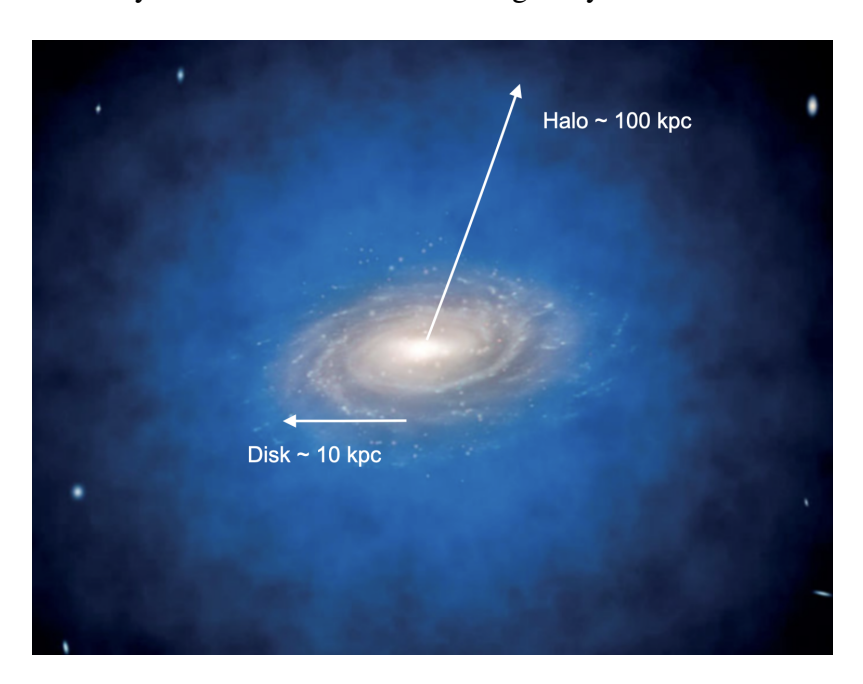


Figure 4: The galactic disk in a dark matter halo (blue). Figure adapted from [4].

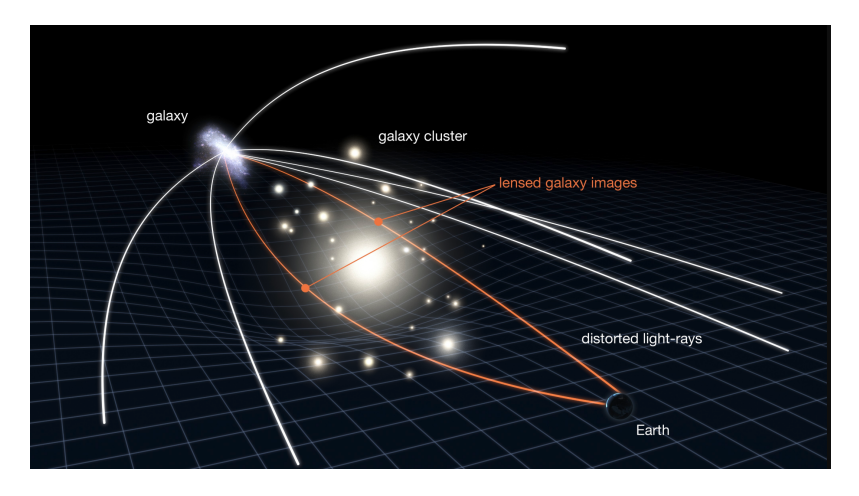


Figure 5: Light deflected by the space-time curvature of massive bodies on its way to earth. Figure from [5].

## 1.2 Gravitational lensing

A good way to distinguish between modified gravity and missing mass is gravitational lensing. This is the effect from light apparently bending its path while following a trajectory in the curved spacetime around massive objects, shown in Figure 5. During the solar eclipse in 1919 the same effect was used to find evidence for general relativity. Today, gravitational lensing has been used to map the mass distributions of galaxies and galaxy clusters. In these measurements there a large amount of missing mass would be required to explain the data, e.g. for the galaxy cluster CL0024+1654 it is 80% missing mass, see Figure 6.

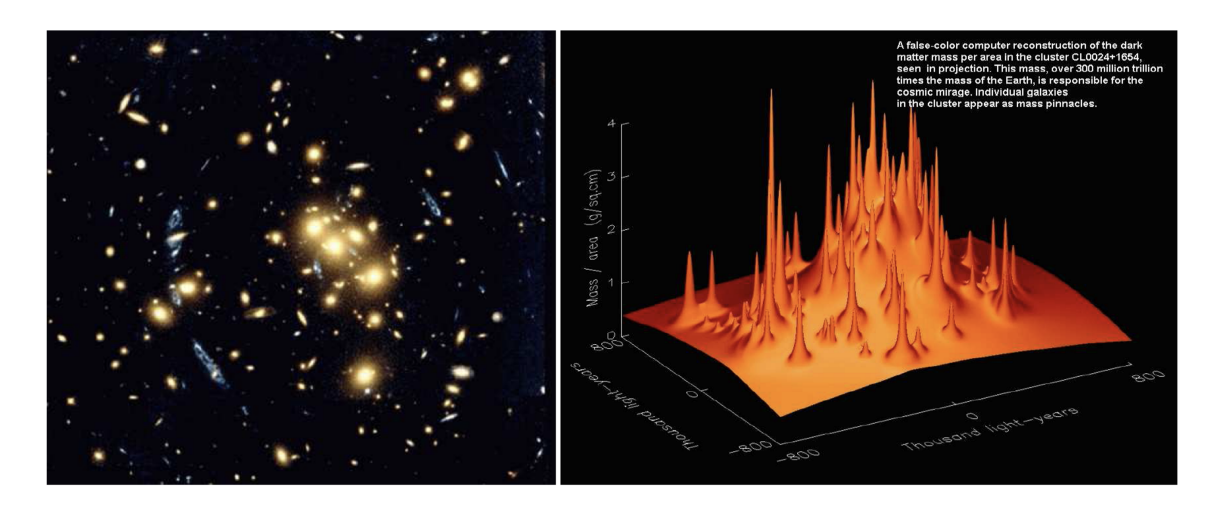


Figure 6: Left: gravitational lensing image with the galaxy cluster CL0024+1654 as the lense. Right: The reconstructed mass distribution. Figure from [6].

### 1.3 Clusters

Not only for stars in galaxies, but also for galaxies in clusters the velocities of orbits can't be explained by Newtonian gravity and the visible mass alone. Historically this was the first sign of dark matter going back to the swiss astronomer Fritz Zwickys observations of the COMA cluster in 1933. The reason this was the first observed effect is that it is really significant. Zwicky suspected the dark matter must be over 99% of the clusters mass. Today, measurements indicate that it is closer to 90%, in line with measurements in many other clusters and with gravitational lensing.

Besides gravitational lensing and orbital measurements, there is a third line of evidence for dark matter in clusters. Observations show that a cluster is composed of three main components: galaxies, hot intracluster gas, and dark matter. Each behaves differently. For example, the gas is heated to tens of millions of degrees and emits strongly in X-rays, allowing astronomers to map its distribution and distinguish it from galaxies and the underlying dark matter. When two galaxy clusters collide, the interaction is dominated by the collision of their enormous hot gas clouds, all embedded within vast halos of dark matter. The gas clouds experience drag and slow down because they interact through electromagnetic forces. In contrast, the dark matter halos pass through one another essentially unaffected, since dark matter does not interact electromagnetically and thus experiences no friction. Because dark matter dominates the total mass of the system, the mass distributions must end up significantly displaced from the centre of the gas clouds. Figure 7 shows a simulation of such a collision in the panels a, b and c. Data from optical and x-rays, as well as from gravitational lensing is shown in Figure 7 d for the case of the Bullet cluster. The fact that most of the mass is outside the gas is difficult to explain with a different gravitational force.

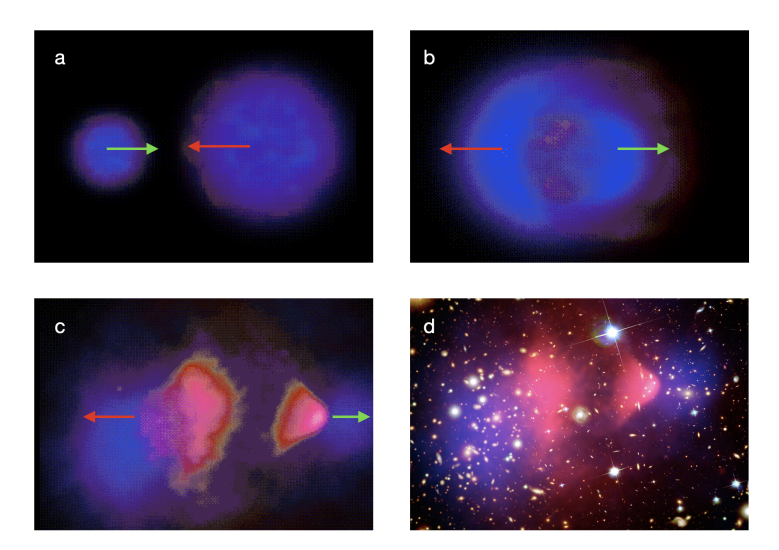


Figure 7: Simulation of the collision of two galaxy clusters modelled as a gas cloud (red) within a dark matter halo (blue). Panel a: the clusters approach each other. Panel b: the dark matter halos move through each other, but the gas experiences friction and heats up. Panel c: The centre-of-mass of each individual cluster has moved significantly further than the gas. Panel d: measured gas and Dark matter distribution after the collision of the Bullet cluster. Figure from [7].

### 1.4 Matter Power spectrum

Matter isn't uniformly distributed in the Universe, it is clumped into galaxies and clusters. The matter power spectrum quantifies the distribution of structure in the Universe at different scales. If we denote the average density of matter as  $\bar{\rho}$ , over- or under-densities as a function of position can be can be measured by

$$\delta(\vec{x}) = \frac{\rho(\vec{x}) - \bar{\rho}}{\bar{\rho}} \,. \tag{5}$$

The two-point correlation function for a distance  $\vec{r} = \vec{x}_1 - \vec{x}_2$  is

$$\xi(|\vec{r}|) = \frac{1}{V} \int d^3x \, \delta(\vec{x}) \delta(\vec{x} + \vec{r}) \,. \tag{6}$$

In the case of the distribution of galaxies,  $\xi(R) > 0$  means there is a higher than random chance to find galaxies separated by r = R. The matter power spectrum is the Fourier transform of the two-point correlation function

$$\xi(r) = \frac{1}{2\pi^2} \int_0^\infty dk P(k) \, \frac{\sin(kr)}{kr} k^2 \, = \frac{1}{2\pi^2} \int_0^\infty dk P(k) \, j_0(kr) k^2 \, , \tag{7}$$

where  $j_0(kr)$  is the zeroth-order spherical Bessel function.

The power spectrum answers the question of whether there is a preferred separation scale between structures in the Universe. For example, in the case of a perfectly uniform Universe, where  $\rho(\vec{x}) = \bar{\rho}$ , it follows that  $\delta(r) = P(k) = 0$ , which means it has no structure at any scale. If there is a special distance R where there is structure and at all other distances it is zero, the correlation function is  $\xi(r) = \delta^{(3)}(r-R)$  and the power spectrum  $P(k) = 4\pi R^2 \sin(kR)/(kR) = 4\pi R^2 j_0(kR)$  oscillates with an oscillation length of  $\pi/R$ . The measured matter power spectrum is shown in Fig. 8. On smaller scales, the Universe was still dominated by radiation when fluctuations began to evolve (more on this later), and radiation pressure suppressed the growth of structure. This leads to a reduction in power at small scales. The position of the turnover depends on the relative amounts of non-relativistic matter and radiation in the Universe. Without dark matter, the turnover would occur at larger scales, and the suppression of small-scale structure would be more pronounced. But there is another feature in the spectrum, a small oscillation just after the turnover point. This means there must be a specific distance at which it is more likely to find galaxies than elsewhere. This distance at about 150 Mpc/h is related to the maximal distance a perturbation could travel in the baryon-photon plasma before atoms formed (recombination). It is very sensitive to the amount of dark matter in the early Universe.

## 1.5 Cosmic Microwave Background

About 380000 years after the Big Bang, the Universe cooled enough for neutral atoms to form and photons were no longer constantly scattered by free electrons in the plasma and began to travel freely through space. These photons have since been redshifted into the microwave regime and are observed today as the cosmic microwave background (CMB)

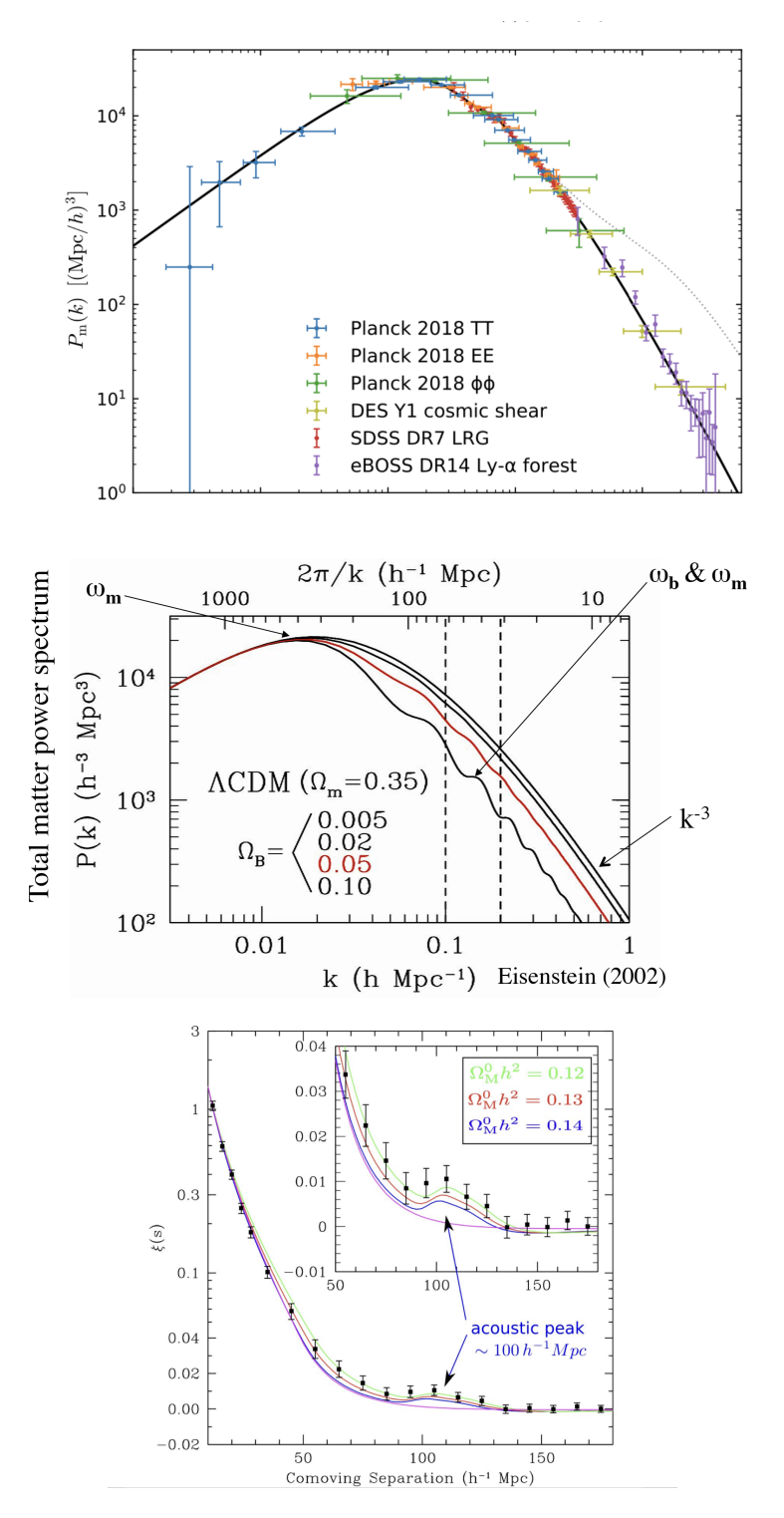


Figure 8: Matter power spectrum of the Universe as measured (upper panel). The middle panel shows the changes to the turnover point if there was more baryonic matter in the early Universe. The lower panel shows the baryon acoustic peak as a function of the two-point correllator. Images taken from [8, 9, 8].

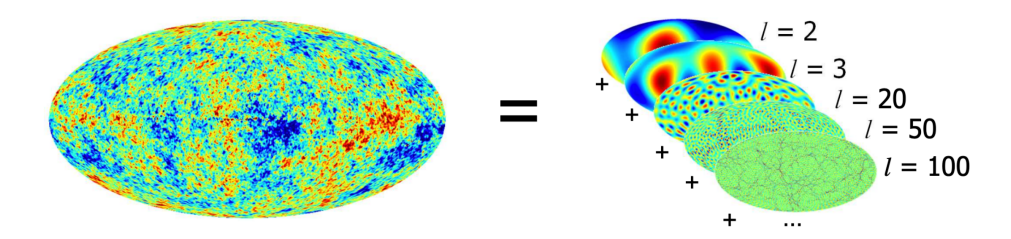


Figure 9: CMB temperature fluctuations decomposed into spherical harmonics. Figure taken from [11].

radiation. The CMB has an almost perfect blackbody spectrum with an average temperature of about 2.7K, and is remarkably uniform, broken only by fluctuations at the microkelvin level. Just like the variations in the large-scale distribution of matter, these tiny anisotropies in the CMB encode a wealth of information about the early Universe and its contents.

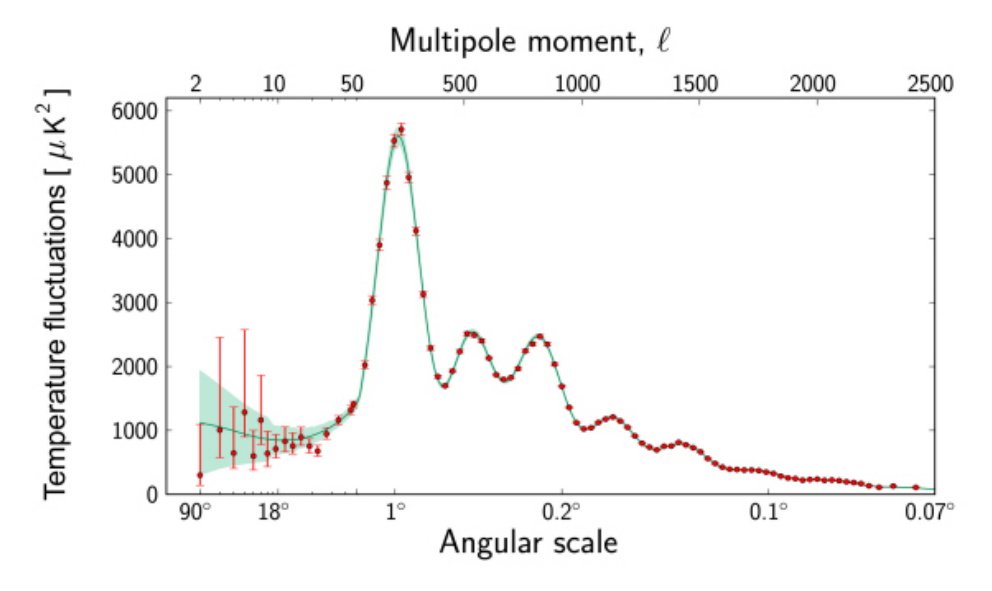


Figure 10: CMB temperature fluctuations decomposed into spherical harmonics. Figure from [12].

Conventionally the CMB temperature fluctuations are represented as a function of angular variables decomposed into spherical harmonics  $Y_{\ell m}(\theta, \phi)$  (familiar from the hydrogen wavefunction),

$$\frac{T(\theta,\phi) - \bar{T}}{\bar{T}} = \sum_{\ell=0}^{\infty} \sum_{m=-\ell}^{\ell} a_{\ell m} Y_{\ell m}(\theta,\phi), \qquad (8)$$

where  $\bar{T}$  is the average temperature. For larger  $\ell$ , spherical harmonics oscillate more rapidly with angle, corresponding to structure on smaller angular scales. This is a generalisation of a Fourier series on a sphere, see Figure 9. In this basis, the CMB measurement

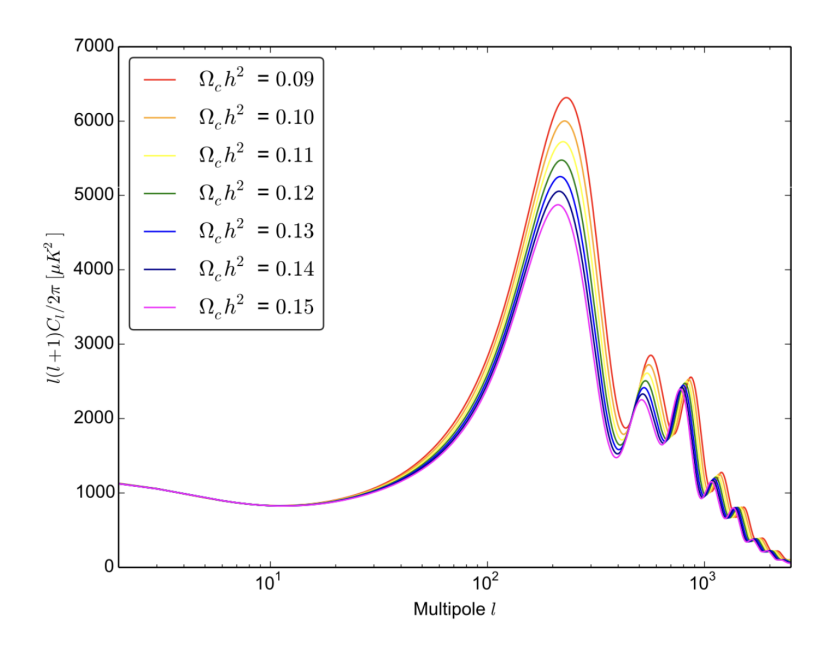


Figure 11: Changes in the CMB for different values of baryonic and dark matter energy densities. Figure from [13].

provides the amplitude of each  $\ell$  component, that is the amount of temperature fluctuations at different angular scales shown in Figure 10. The position of the peaks of the CMB encodes information about the geometry of the Universe and its matter content. They are caused by the acoustic oscillations in the primordial plasma and correspond to the oscillation modes that have compressed once (first peak), compressed and decompressed once (second peak) compressed, decompressed and compressed again (third peak), etc. At the time the CMB formed the Universe was roughly 1\% of the sky today. This corresponds to a value of  $\ell \approx \frac{\pi}{4} \approx 220$ . If the Universe wasn't flat, but curved one would expect  $\ell > 200$  or  $\ell < 200$ , because the CMB light would've been bend further apart (closed Universe) or closer together (open Universe) on he way here. The CMB measurement shows it very close to spatially flat. The amount of matter also has an effect on these oscillations. In the competition between radiation pressure and gravity in the primordial plasma, dark matter contributes only to the gravitational side, as it does not interact with light and thus exerts no radiation pressure. This imbalance strengthens the compression phases of the acoustic oscillations while leaving the rarefaction phases relatively weaker. Since higherorder odd-numbered peaks in the CMB correspond to modes that have undergone multiple compressions, the cumulative influence of dark matter amplifies these peaks relative to the even peaks. As a result, the presence of more dark matter leads to increased amplitude in the higher odd peaks, as illustrated in Figure 11.

## 1.6 Properties of Dark Matter

We have seen evidence for the existence of additional matter at scales ranging from galaxies (10 kpc) to the whole Universe. Taken together, these observations allow us to infer

several key properties that any new physics must possess to account for these phenomena. A viable dark matter candidate must be

- neutral: If dark matter was charged it would contradict many observations. If it had charges large enough to clump efficiently this would change the Halo shape significantly. But there are even bounds on small charges. In galaxy cluster collisions, any charge would lead to friction and the dark matter halos wouldn't pass through each other as observed. Currently the bound on any electric charges is

$$q_{\rm DM} \lesssim 10^{-4} \left(\frac{m_{\rm DM}}{\rm TeV}\right)^{1/2} \tag{9}$$

- **cold:** Dark matter must have been non-relativistic since the early Universe in order to account for the observed features of the cosmic microwave background and the matter power spectrum. If dark matter had been relativistic during the epoch of acoustic oscillations in the photon-baryon plasma, it would not have acted as an effective source of gravitational potential wells. For thermal dark matter that has been in equilibrium with the primordial plasma one can even constrain the mass from this argument  $m_{\rm DM}^{\rm th} > 2$  keV. For dark matter to explain galaxy rotation curves today, it must move more slowly than the typical escape velocity of galaxies. Otherwise, the dark matter would not remain gravitationally bound to halos and could not account for the observed flat rotation curves.
- **stable:** If dark matter is responsible for effects in the early Universe and still contributes to gravitational lensing effects and galactic rotation curves today, it must be stable. This doesn't mean absolutely stable, but we can use the lifetime of the Universe to set a bound on it's decay width

$$\Gamma_{\rm DM} \times 1.3 \times 10^{10} \, {\rm yrs} \gtrsim 1 \,.$$
 (10)

- non-baryonic: One could speculate whether it would be possible to have composite dark matter made from quarks and gluons, like the neutron, which would have many of the required properties. In addition, the observation that the energy density of baryonic matter and dark matter is relatively close  $\Omega_{\rm DM} \approx 5 \times \Omega_b$  could be considered a hint for a common origin. However, a major challenge arises from the epoch of nucleosynthesis in the early universe. If such dark matter particles were present during the formation of light elements, they would have interacted with the nucleons and light nuclei, such as deuterium. Scattering processes would have altered the standard reaction rates and reduced the predicted abundance of deuterium. Since the observed deuterium abundance matches standard Big Bang Nucleosynthesis predictions remarkably well, this places stringent constraints on any dark matter candidate with such interactions.
- **collisionless:** Even though dark matter can't interact strongly with Standard Model particles, in principle it could interact with itself. There could even be a whole dark sector of particles and interactions similar to what we observe in visible matter.

However, for similar reasons that constrain dark matter electric charges, these self-interactions need to be small. Otherwise the galaxy cluster collisions would lead to friction between the dark matter halos. Currently the bound on the cross section is

$$\frac{\sigma}{m_{\rm DM}} \le 1 \frac{\rm cm^2}{\rm gr} \,. \tag{11}$$

### **Lecture 2: Dark Matter Candidates**

If we go through the Standard Model of particle physics we don't find a candidate that has all the properties described in the last Section. Only stable, massive particles are an option, which excludes everything apart from electrons, protons, neutrinos and other composite states. In fact, the neutrino almost has all the right properties. Why can't the neutrino be dark matter? To understand that we repeat some Cosmology.

### 2.1 Cosmology

The Universe expands, which can be parameterised by a scale factor a(t). Any length scale  $\ell_0$  stretches to the new scale  $\ell(t) = a(t)\ell_0$  after a time t. This of course is only true in a perfectly homogeneous, isotropic Universe. Local forces will affect the motion and a pair of galaxies separated by a distance d is separated by  $x(t) = a(t)d + \delta x$  after a time t, where  $\delta x$  would be local motion for example in a gravitational well like a cluster. One can then define the rate at which objects become more distant from each other as a result of the expansion of the universe, the *recessional velocity*,

$$\frac{dx(t)}{dt} = v = \dot{a}(t)d = \frac{\dot{a}(t)}{a(t)}a(t)d = H(t)x(t). \tag{12}$$

Here H(t) is the Hubble rate and its value today is

$$H_0 = \frac{\dot{a}(t_{\text{today}})}{a(t_{\text{today}})} = 70 \frac{\text{km}}{\text{s Mpc}}.$$
 (13)

It measures the current expansion rate of the Universe. One can use it to define the Hubble horizon, which is the furthest distance over which causal processes can operate within one Hubble time

$$R_{\rm H} = \frac{c}{H_0} \,. \tag{14}$$

If you solve the Einstein equations for spatially homogeneous and isotropic Universe that is allowed to expand or contract over time one can derive how the expansion

rate depends on the density if the Universe has no spatial curvature, the Friedmann equation

$$H(t)^2 = \frac{\rho_c}{3M_{\rm Pl}^2} \,, \tag{15}$$

where  $M_{\rm Pl}$  is the Planck scale and  $\rho_c$  is the *critical density* for a flat Universe. To understand how the Hubble rate changes with time we need to understand how the density of the Universe changes with time.

We can decompose all matter and radiation in the Universe into three components, non-relativistic matter, relativistic bosons and relativistic fermions. Relativistic and non-relativistic means that the mass of the particle is small compared to the temperature. The energy density can then be written as a function of the temperature as

$$\rho(T) = g \int \frac{d^3p}{(2\pi)^3} \frac{E}{e^{E/T} \pm 1} = \begin{cases} mg \left(\frac{mT}{2\pi}\right)^{3/2} e^{-m/T}, & T \ll m, \\ \frac{\pi^2}{30} g T^4, & \text{bosons } (T \gg m), \\ \frac{7}{8} \cdot \frac{\pi^2}{30} g T^4, & \text{fermions } (T \gg m), \end{cases}$$
(16)

where g is the number of degrees of freedom, e.g. photons have two polarisations and  $g_{\gamma}=2$ . The scaling of the density for relativistic particles follows directly from dimensional analysis because  $T\gg m$  and  $\rho\sim T^4$ . The density of relativistic matter falls off with  $T^4$  when the Universe cools, but non-relativistic matter contributions fall off with  $e^{-m/T}$ . We can neglect them to very good approximation. For completeness we also give the number density, which is defined analogously to  $\rho(T)$  apart from the factor E in the numerator of the integrand and scales like  $T^3$  for relativistic species, so that

$$n(T) = g \int \frac{d^3p}{(2\pi)^3} \frac{1}{e^{E/T} \pm 1} = \begin{cases} g \left(\frac{mT}{2\pi}\right)^{3/2} e^{-m/T}, & T \ll m, \\ \frac{\zeta_3}{\pi^2} g T^3, & \text{bosons } (T \gg m), \\ \frac{3}{4} \cdot \frac{\zeta_3}{\pi^2} g T^3, & \text{fermions } (T \gg m). \end{cases}$$
(17)

This allows us to write the critical density as a function of time,

$$\rho_c(T) = \frac{\pi^2}{30} g_{\text{eff}}(T) T^4 \,, \tag{18}$$

where

$$g_{\text{eff}}(T) = \sum_{\text{bosons}} g_B \frac{T_B^4}{T^4} + \frac{7}{8} \sum_F g_F \frac{T_F^4}{T^4}.$$
 (19)

The number of effective degrees of freedom changes with time (or temperature). At the time of the CMb for example only photons and neutrinos were relativistic and the number of effective degrees of freedom was

$$g_{\text{eff}}(T_{\text{CMB}}) = 2_{\gamma} + \frac{7}{8} N_{\nu}^{\text{rel}} \frac{T_{\nu}^{4}}{T^{4}} = 2_{\gamma} + \frac{7}{8} N_{\nu}^{\text{rel}} \left(\frac{4}{11}\right)^{4} \approx 3.36$$
 (20)

for  $N_{\nu}^{\rm rel}=3$ . Figure 14 shows how  $g_{\rm eff}$  changes with time.

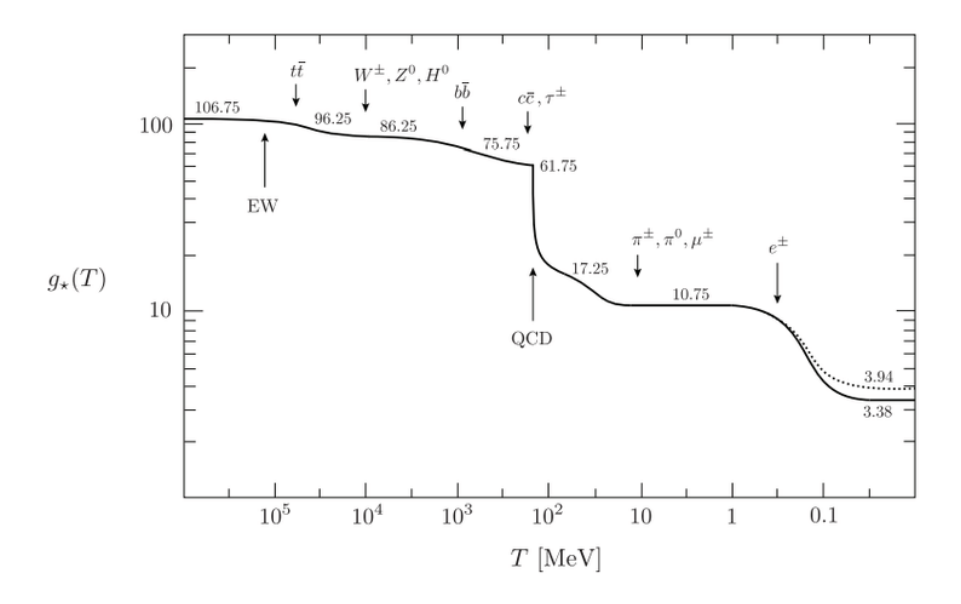


Figure 12: Number of effective degrees of freedom as a fucntion of the temperature of the Universe. Figure from [14].

# 2.2 The Origin of Species

In the early Universe, the hot and dense plasma kept all Standard Model particles in thermal equilibrium through frequent interactions. The interaction rate for a given species depends on its interaction cross section, the relative velocity between particles, and the number density of available interaction partners

$$\Gamma = \sigma \cdot v \cdot n \,. \tag{21}$$

Since the particles are relativistic we can set c=1 from now on. A particle species remains in thermal equilibrium until the temperature of the plasma reaches the decoupling temperature  $T=T_{\rm dec}$ ,

$$H(T_{\text{dec}}) = \Gamma(T_{\text{dec}}). \tag{22}$$

The right hand side takes input from particle physics to calculate the cross section  $\sigma$  and he number density follows from (16) and needs astrophysics input. For example the density of electrons in the primordial plasma scales like

$$n_e = \frac{2}{\pi^2} T_{\text{dec}}^3 \tag{23}$$

Using equation (22) we can calculate for example the temperature and age of the Universe when neutrinos decoupled from the thermal plasma. Neutrinos interact via the weak interaction with the standard model particles, so that the cross section scales like

$$\sigma_{\nu e \to \nu e} \approx G_F^2 T_{\text{dec}}^2 \,,$$
 (24)

We can now use (18) to write

$$H(T) = \Gamma(T) \tag{25}$$

$$\left(\frac{\pi^2}{30}g_{\text{eff}}(T)\frac{T^4}{3M_{\text{Pl}}^2}\right)^{1/2} = G_F^2 T^2 \left(\frac{2}{\pi^2}T^3\right)$$
(26)

$$\Rightarrow T^3 = \pi \sqrt{\frac{g_{\text{eff}}(T)}{90}} \frac{1}{M_{\text{Pl}}G_F^2}$$
 (27)

$$\approx \frac{\pi}{\sqrt{9}} \frac{1}{M_{\rm Pl} G_F^2} \approx 10^{10} {\rm GeV}^4 \frac{1}{10^{19} {\rm GeV}}$$
 (28)

$$\approx 10^{-9} \,\text{GeV}^3\,,\tag{29}$$

using  $g_{\rm eff}(T_{\rm dec}) \approx 10$  and the neutrinos decouple when the Universe had a temperature of

$$T_{\rm dec}^{\nu} \approx 1 \,{\rm MeV}$$
 (30)

Using the Hubble rate at this temperature and the neutrinos decoupled from the thermal bath when the Universe was 1 s old,

$$t = \frac{1}{2H(T_{\text{dec}}^{\nu})} \approx 1\text{s}. \tag{31}$$

we can calculate todays density of neutrinos, which by now are non-relativistic so that

$$\rho_{\nu} = m_{\nu} n_{\nu} (T_0) = \frac{3}{4} \frac{2\zeta_3}{\pi^2} T_{\nu}^3 = m_{\nu} \frac{6}{11\pi^2} T_{0,\gamma}^3, \tag{32}$$

and  $T_{0,\gamma}=2.4\cdot 10^{-4}~{\rm eV}$  is the temperature of the cosmic microwave background. The contribution to the energy density in the Universe from any species is defined as  $\Omega_i h^2=\rho_i/\rho_c(H^*)$ , where the critical density is fixed at  $H^*=100\,{\rm km/s/Mpc}$  so that  $\rho_c(H^*)=8.1\cdot 10^{-11}\,{\rm eV}^4$ . The contribution from the neutrino density is

$$\Omega_{\nu}h^{2} = m_{\nu} \frac{6}{11\pi^{2}} \frac{T_{0,\gamma}^{3}}{\rho_{c}(H^{*})} 
= \frac{m_{\nu}}{18} \frac{(2.4 \cdot 10^{-4})^{3}}{8.1 \cdot 10^{-11}} \frac{1}{\text{eV}} 
= \frac{m_{\nu}}{105 \,\text{eV}},$$
(33)

whereas the measured dark matter relic density is

$$\Omega_{\rm DM}h^2 = 0.1198 \pm 0.0012. \tag{34}$$

We know the neutrino mass is below  $m_{\nu} \lesssim 1 \mathrm{eV}$ , so they can't explain dark matter. But we can turn the equation around and ask what kind of particle  $\chi$  would we need to explain the relic density. The freeze-out condition reads

$$\Gamma = \sigma_{\chi\chi} v n_{\chi} = \frac{\pi}{\sqrt{90} M_{\rm Pl}} \sqrt{g_{\rm eff}} T^2 \,, \tag{35}$$

so that the number density at the time of decoupling can be written as

$$n_{\chi}(T_{\text{dec}}) = \frac{\pi}{\sqrt{90}M_{\text{Pl}}} \sqrt{g_{\text{eff}}(T_{\text{dec}})} \frac{T_{\text{dec}}^2}{\sigma_{\chi\chi}v}.$$
 (36)

For the relic abundance of dark matter today follows

$$\Omega_{\rm DM}h^{2} = \frac{m_{\chi}n_{\chi}(T_{0})}{\rho_{\rm c}(H^{*})} 
= \frac{m_{\chi}}{\rho_{\rm c}(H^{*})} \left(\frac{a(T_{\rm dec})}{a(T_{0})}\right)^{3} n_{\chi}(T_{\rm dec}) 
= \frac{m_{\chi}}{\rho_{\rm c}(H^{*})} \left(\frac{a(T_{\rm dec})T_{\rm dec}}{a(T_{0})T_{0}}\right)^{3} \frac{T_{0}^{3}}{T_{\rm dec}^{3}} n_{\chi}(T_{\rm dec}) 
= \frac{m_{\chi}}{\rho_{\rm c}(H^{*})} \frac{T_{0}^{3}}{T_{\rm dec}^{3}} \frac{\pi}{\sqrt{90}M_{\rm Pl}} \frac{g_{\rm eff}(T_{0})}{\sqrt{g_{\rm eff}(T_{\rm dec})}} \frac{T_{\rm dec}^{2}}{\sigma_{\chi\chi}v} 
= \frac{T_{0}^{3}}{M_{\rm Pl}\rho_{\rm c}(H^{*})} \frac{\pi}{\sqrt{90}} \frac{g_{\rm eff}(T_{0})}{\sqrt{g_{\rm eff}(T_{\rm dec})}} \frac{x}{\sigma_{\chi\chi}v},$$
(38)

which is largely insensitive to the dark matter mass and inversely proportional to the cross section. Note that we used  $x \equiv m_\chi/T_{\rm dec}$ , and  $n_\chi(T_{\rm dec})a(T_{\rm dec}) = n_\chi(T_0)a(T_0)$  and  $g_{\rm eff}(T_0)T_0^3a(T_0)^3 = g_{\rm eff}(T_{\rm dec})T_{\rm dec}^3a(T_{\rm dec})^3$  and  $g_{\rm eff}(T_{\rm dec}) \approx 100$  and  $g_{\rm eff}(T_0) = 3.36$ . Anticipating  $x \approx 23$  we find for the cross section

$$\langle \sigma_{\chi\chi} v \rangle = 3.6 \cdot 10^{-10} \,\text{GeV}^{-2} = 4.2 \cdot 10^{-27} \,\text{cm}^3/\text{s} \,.$$
 (39)

Note that this is an approximation to the full calculation which requires to solve the Boltzmann equation and yields a cross section a factor few larger. Also in general the cross section enters as a thermal average, which becomes relevant when the interaction cross section has a velocity dependence,

$$\langle \sigma v \rangle = \frac{\int d^3 p_1 \, d^3 p_2 \, f(p_1) \, f(p_2) \, \sigma v}{\int d^3 p_1 \, d^3 p_2 \, f(p_1) \, f(p_2)} \approx a + \frac{6b}{x}, \quad \text{for} \quad \sigma v = a + bv, +\mathcal{O}(v^4).$$
 (40)

Since dark matter needs to be cold already in the early Universe, we also have

$$\Gamma = \sigma_{\chi\chi} v n_{\chi}$$

$$= \sigma_{\chi\chi} \sqrt{\frac{2T}{m_{\chi}}} g_{\text{eff}} \left(\frac{m_{\chi} T}{2\pi}\right)^{3/2} e^{-\frac{m_{\chi}}{T}} = \frac{\pi}{\sqrt{90} M_{\text{Pl}}} \sqrt{g_{\text{eff}}} T^2$$
(41)

where we used  $v = \sqrt{2T/m}$ . It follows that

$$x = \log \left[ \frac{m_{\chi} M_{\text{Pl}} \sqrt{90}}{\sqrt{g_{\text{eff}} \pi^{5/2}}} \sigma \right]$$
 (42)

depends only logarithmically on the DM mass. Assuming a electroweak cross section

$$\sigma = \frac{\pi \alpha^2 m_\chi^2}{c_w^4 M_Z^4} \tag{43}$$

we find

$$x = \log \left[ \frac{\sqrt{90}}{\sqrt{g_{\text{eff}}}} \frac{\alpha^2}{c_w^4 \pi^{3/2}} \frac{m_{\chi}^3 M_{\text{Pl}}}{M_Z^4} \right]$$
 (44)

which yields  $x\approx 21-28$  for  $m_\chi=10-100$  GeV. This is called the Weakly Interacting Massive Particle (WIMP) miracle, because a dark matter candidate with a weak-scale coupling strength and a weak scale mass has the right properties to explain the observed relic abundance.

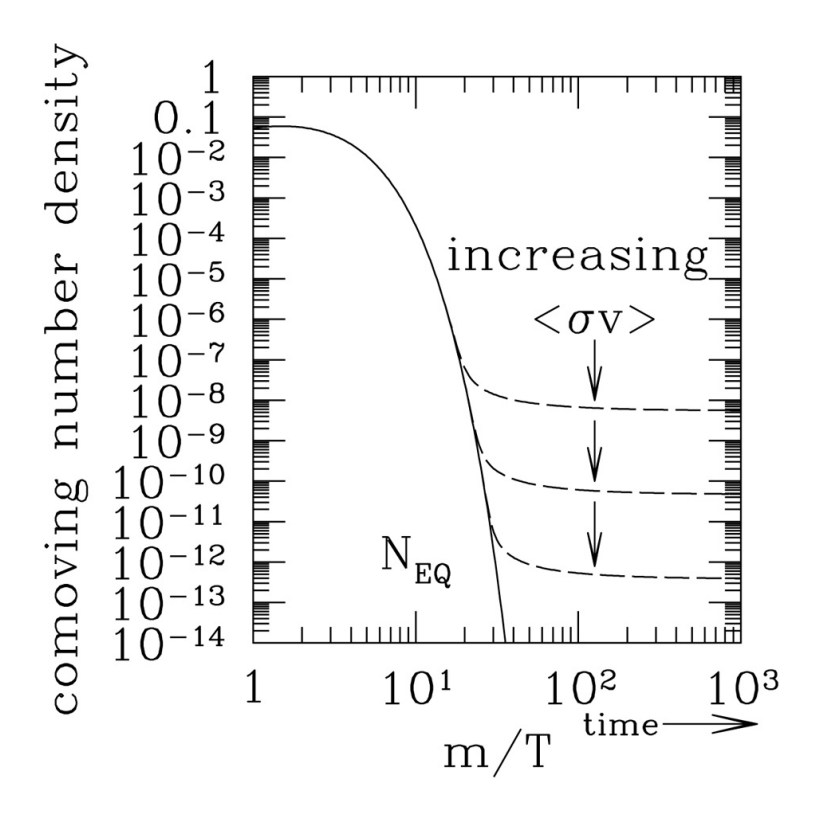


Figure 13: Freeze-out of dark matter as a function of x for different values of the interaction cross section. Figure from [15].

### **Lecture 3: Dark Matter Detection**

Dark matter that has been in thermal equilibrium needs to interact with the Standard Model strongly enough to fulfil equation (??). It is the same way the abundance of all SM particles can be explained (although we haven't detected the Cosmic Neutrino Background at the time of writing), and some people consider it a motivating fact that the relic abundance of dark matter  $\Omega_{\rm DM}h^2$  and baryonic matter  $\Omega_Bh^2$  are of similar order of magnitude (instead of many, many orders of magnitude apart). But Dark Matter could be entirely different, freezing in instead of freezing out, or an almost classical field, e.g. an axion, or even primordial black holes. This section will focus on the detection techniques for thermal dark matter and at the end comment on approaches to discover dark matter that never was in thermal equilibirum.

#### 3.1 Direct Detection

Direct detection experiments are laboratory searches for dark matter interacting with a target. A large target mass and good shielding are important to maximise sensitivity and suppress background noise. Therefore, state-of-the-art experiments use multi-ton noblegas detectors (xenon or argon) located deep underground, often in former mines, to reduce cosmic-ray backgrounds. A limiting factor for direct detection experiments is the recoil energy of the target nucleus, which is determined by the momentum transferred during the scattering process. Since dark matter particles are non-relativistic, the momentum transfer and therefore the recoil energy depend on dark matter mass and velocity,

The velocity of DM needs to be below the escape velocity of the galaxy  $v_{\rm esc}\approx 550$  km/s to stay gravitationally bound. Dark matter particles are therefore non-relativistic and have a speed of  $v\approx 10^{-3}c$  and a momentum of p=mv. In an elastic collision the recoil energy of the target nucleus is given by

$$E_R = \frac{|\vec{q}|^2}{2m_N} = E_\chi \eta \frac{1 - \cos \theta}{2}, \quad \text{and} \quad \eta = \frac{4\mu^2}{m\chi m_N} = \frac{4m_\chi m_N}{(m_\chi + m_N)^2}, \quad (45)$$

where  $E_\chi=1/2m_\chi v^2$  is the kinetic energy of the dark matter particle and  $\mu$  is the reduced mass. In terms of the Dark Matter mass

$$E_R = 10 \,\text{keV} \left(\frac{m_\chi}{20 \,\text{GeV}}\right) \left(\frac{100 \,\text{GeV}}{m_N}\right) \,, \tag{46}$$

where 10 keV is roughly the threshold recoil energy of Xenon-based detectors. The differential event rate can then be written as

$$\frac{dR(E_R)}{dE_R} = n_{\chi} \int_{v_{\min}}^{v_{\text{esc}}} v f(v) \frac{d\sigma}{dE_R} dv = n_{\chi} \int_{v_{\min}}^{v_{\text{esc}}} v e^{-v^2/v_0^2} dv \propto n_{\chi} e^{-E_R/E_0} , \qquad (47)$$

where  $v_0$  is the average speed and  $v_{\min} = \sqrt{2E_R/(\eta m_\chi)}$ . Figure ?? shows a typical explains the exclusion contours of direct detection bounds. At the lower mass limit it is set by the exponential recoil suppression and towards higher masses by the reduced number density  $n_\chi = \rho_\chi/m_\chi$ .

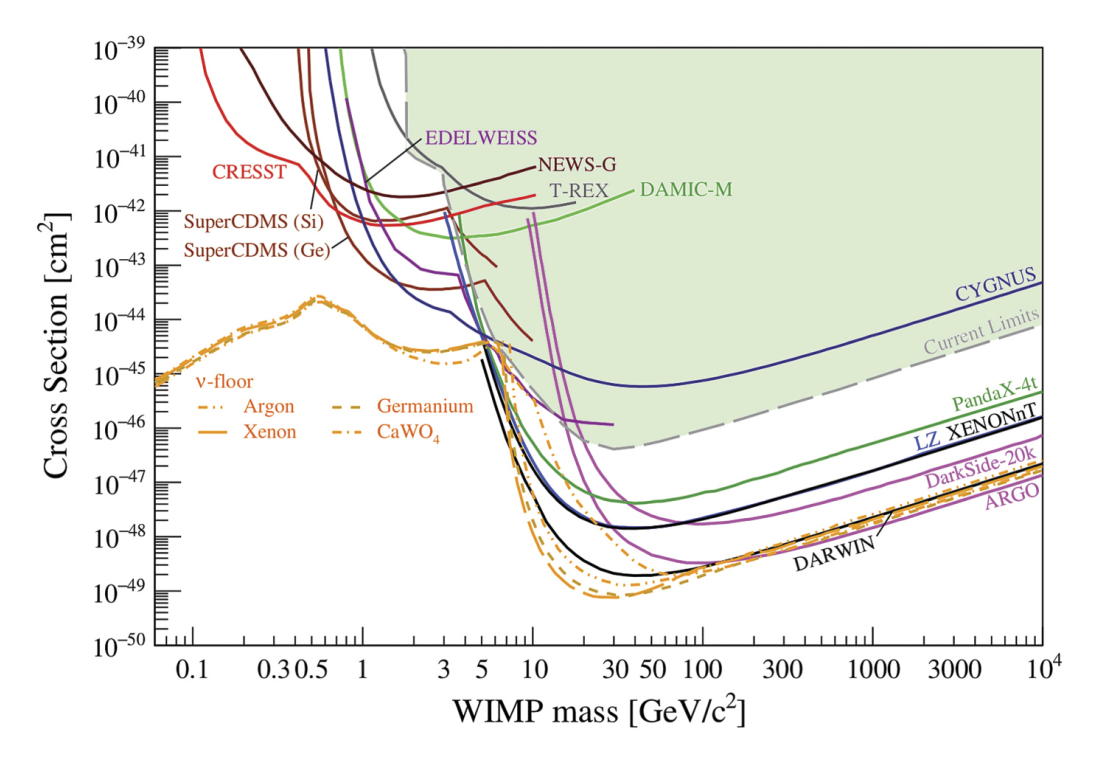


Figure 14: Sensitivity contours from direct detection experiments (coloured, solid contours). The orange contours denote the 'neutrino fog', below which the experiments become sensitive to solar neutrino coherent scattering. Figure taken from [16].

### 3.2 Indirect Detection

If both dark matter and dark antimatter exist today, they can annihilate into Standard Model particles, e.g.  $\chi \bar{\chi} \to \gamma \gamma$ . This is expected for thermally produced dark matter, as discussed in Section 2.2. However, dark matter need not be symmetric. Just as visible matter exhibits a baryon-antibaryon asymmetry, scenarios such as asymmetric dark matter allow for an imbalance between dark matter and its antiparticle. If dark matter annihilates it happens most likely were the dark matter density is high. Typical searches are therefore satellites looking for energetic photons from the centre of the galaxy.

In the annihilation of two dark matter particles into photons, each photon in the final state carries energy  $E_{\gamma}=m_{\chi}$  up to non-relativistic corrections. In case they annihilate into different final states, photons can be produced from final state radiation or decays of final state particles such that  $E_{\gamma} < m_{\chi}$ . The energy dependence of the photon flow reads

$$\frac{d\phi(E_{\gamma})}{dE_{\gamma}} = \frac{1}{4\pi} \frac{\langle \sigma v_{\text{rel}} \rangle}{2m_{\chi}^2} \frac{dN_{\gamma}}{dE_{\gamma}} J = \frac{\Gamma}{4\pi m_{\chi}} \frac{dN_{\gamma}}{dE_{\gamma}} \int d\Omega \int_{\text{los}} \rho_{\chi}^2 d\ell \,, \tag{48}$$

where 'los' denotes the 'line of sight', the distance from the observer to the annihilation event and  $N_{\gamma}$  the number of photons per annihilation event. Dark matter can annihilate independent of its mass, and for lighter dark matter annihilation is more likely since the flux scales like  $\rho_{\chi}^2$ . However, for dark matter with masses at or below the MeV scale, backgrounds like the diffuse galactic emissions make it difficult to constrain the signal. In Figure 15 shows limit from different indirect detection searches for  $\chi \bar{\chi} \to b \bar{b}$  annihilation.

The annihilation cross section is the same that appears in the thermal abundance calculation in Section 1.6, so that the parameter space where the cross section is equal (or smaller in case its a fraction of Dark Matter) than is shown in Figure 15 as 'Thermal WIMP cross section'.

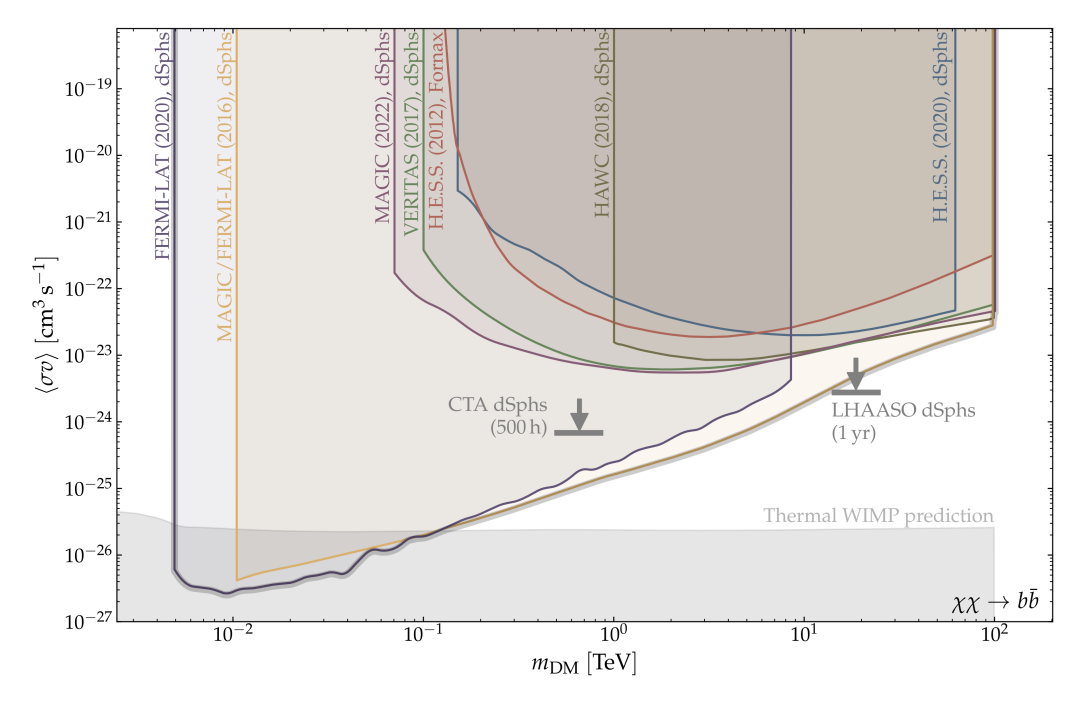


Figure 15: Bounds from indirect detection searches for dark matter annihilating into b quarks  $\chi\bar{\chi}\to b\bar{b}$ . Figure taken from [17]. Here the lower limit is set by the mass of the b quark, in searches for  $\chi\bar{\chi}\to\gamma\gamma$  it can be as low as  $\sim$  MeV.

#### 3.3 Collider searches

Both direct and indirect detection are limited by the mass of dark matter. If dark matter is too light it doesn't have enough momentum to produce recoil in direct detection targets or produces photons too soft to be detected over the background in indirect detection. Colliders can overcome this limitation because dark matter can be produced with large momentum. The relevant process at colliders is the production of dark matter together with a SM particle. Just like neutrinos, dark matter would pass through the detector invisibly, whereas the SM particles, be it a jet, photon, lepton, etc., can be detected. The transverse momentum of the SM particle is then unbalanced. The signal events are then single SM particles together with missing energy, they're called mono-jet, mono-photon, etc. There is an additional advantage of the potential production of dark matter at colliders. Since dark matter particles in the halo are non-relativistic, interactions with the SM are typically suppressed by the mediator mass, see (24) and (43). The reason is that the momentum in these interactions is much smaller than the mass of the mediator and only the leading term

of the propagator enters the calculation of the cross section

$$\frac{g^2}{p^2 - M^2} = -\frac{g^2}{M^2} - \frac{g^2 p^2}{M^4} + \dots {49}$$

At a collider however the mediator can be produced on resonance  $p^2 \approx M^2$ , if it isn't too heavy. This resonant enhancement can lead to substantially enhanced cross section as compared to direct and indirect detection. The production cross section at colliders is also independent of the details of the dark matter halo. Therefore any possible observation could only be linked to dark matter in a specific model. A very simple model is the Higgs portal, which only adds a single scalar  $\chi$  as a dark matter candidate interacting with the Higgs boson via the operator

$$\mathcal{L} = -\frac{\lambda}{2} \chi^2 H^{\dagger} H ,. \tag{50}$$

This leads to the Higgs decay  $h \to \chi \chi$  with a decay rate

$$\Gamma(h \to \chi \chi) = \frac{\lambda^2}{32\pi} \frac{v^2}{M_h} \sqrt{1 - \frac{4m_\chi}{M_h^2}}.$$
 (51)

If the Higgs boson is produced in association with a gauge boson  $q + \bar{q} \to hZ$  or in vector-boson fusion  $q + \bar{q} \to q' + \bar{q}' + h$  (where q' is down-type if q is up-type and vice versa), one can detect this signal at colliders. At the same time the direct detection cross section is sensitive to the same parameters, but suppressed by the Higgs mass

$$\sigma = \lambda^2 \frac{f_N^2}{4\pi} \frac{\mu m_N^2}{m_\gamma^2 M_h^4} \,. \tag{52}$$

Dark matter annihilation and the freeze-out of dark matter in the early Universe are proportional to the same parameters. For this simple model the corresponding parameter space is shown in Figure 16. The features discussed in this section can be identified in this figure. The low-mass threshold and the suppression of the cross section at higher masses by the dark matter density for in the case of both direct and indirect detection, as well as the mass independence of the constraints from invisible Higgs searches. The Higgs pole structure of the annihilation cross section can also be seen in the contour for constant relic abundance around  $m_\chi = M_h/2$ .

#### 3.4 Searches for non-thermal dark matter

If dark matter wasn't in thermal equilibrium with the standard model plasma in the early Universe, the relic abundance isn't explained by the freeze-out condition. As a result the dark matter mass and couplings to standard model particles aren't constrained by the freeze-out condition either. However, any candidate must still check all the boxes listed in Section 1.6, in particular it must have been non-relativistic already in the early Universe. A few candidates worth mentioning

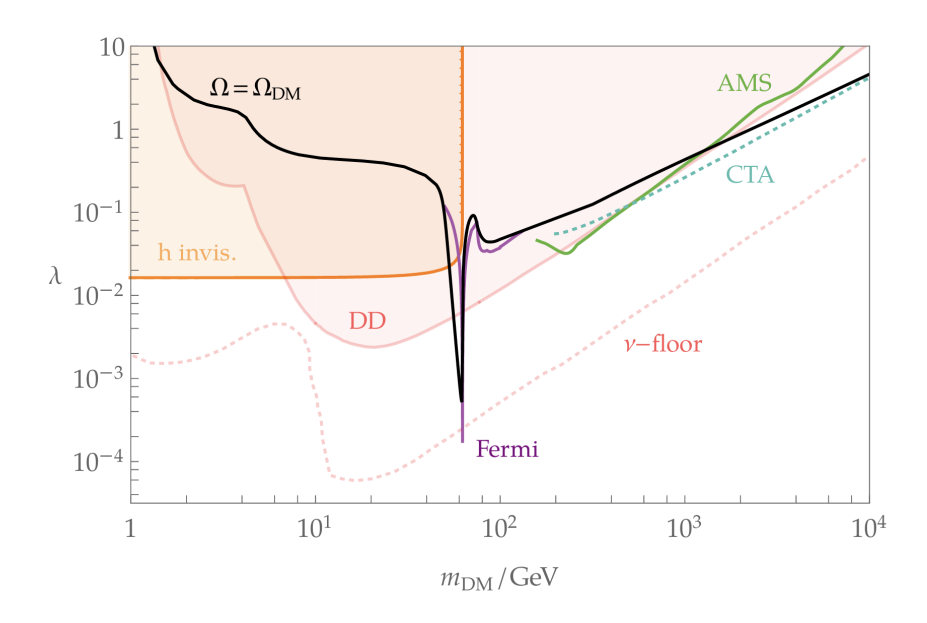


Figure 16: Bounds from collider, direct and indirect detection searches for dark matter interacting with the SM via the Higgs portal. Figure taken from [18].

- Freeze-in dark matter is produced by the decay of a mediator particle that is very weakly coupled to the Standard Model bath. In this scenario, the dark matter particles never reach thermal equilibrium with the plasma; instead, their relic abundance is built up gradually as the mediator undergoes rare decays (or scatterings) into the dark sector. Since the interaction strength is typically feeble, the production is most efficient at early times when the mediator is abundant, and it shuts off as the Universe expands and the mediator population becomes Boltzmann suppressed. Freeze-in dark matter is so feebly interacting that it is probed indirectly via the properties and lifetimes of the mediator particle, such as displaced decays or deviations in cosmological observables
- Asymmetric dark matter is the idea that the dark sector has an asymmetry similarly to the asymmetry between matter and anti-matter in the SM. In this framework, the relic abundance of dark matter is not set by thermal freeze-out but rather by the primordial asymmetry between dark matter and anti-dark matter particles. The symmetric component annihilates efficiently in the early Universe, leaving behind a net excess whose density is naturally comparable to the baryon density. This connection provides a possible explanation for the observed coincidence ( $\Omega_{\rm DM} \sim 5\,\Omega_b$ , suggesting a common origin of visible and dark matter. Unlike symmetric WIMP scenarios, asymmetric dark matter is not expected to produce significant indirect detection signals from annihilation today.
- Ultralight dark matter can only be realised for bosons, because fermion dark matter masses are constrained by the Pauli exclusion principle and the total halo mass. As a consequence of the misalignment mechanism and the high occupation number, this type of dark matter is best described by a classical wave  $\phi(x,t) =$

 $\frac{\sqrt{2
ho_{
m DM}}}{m_\phi}\sin{(\omega t+\delta)}$ . This dark matter can be so light  $m_\phi<10^{-20}$  eV, and so weakly coupled that none of the strategies discussed here are sensitive. It's interactions with SM particles could be observed in modifications of fundamental constants, e.g. the interaction

$$\mathcal{L} = -m_e \bar{\psi}_e \psi_e - m_e \frac{\phi}{\Lambda} \bar{\psi}_e \psi_e \tag{53}$$

$$\Rightarrow m_e(\phi) = m_e \left( 1 + \frac{1}{\Lambda} \frac{\sqrt{2\rho_{\rm DM}}}{m_\phi} \sin(\omega t + \delta) \right)$$
 (54)

leads to a time-dependent, oscillating electron mass that would induce time-dependent transition frequencies in atomic clocks. A particularly famous candidate for ultralight dark matter is the axion, because the axion has a reason to be small. At leading order the pseudoscalar axion interactions don't lead to oscillating constants. Experimental techniques to search for axions are cavity searches and light-shining-through a wall searches, which take advantage of the fact that axions interacting with photons induces interactions with a magnetic field B such that  $a+\gamma^*\to\gamma$  of a wavelength dictated by the axion mass and  $\gamma^*$  is the virtual photon from the B field.

- Primordial black holes are dark matter candidates that are produced in the early Universe from the direct gravitational collapse of large density fluctuations, phase transitions, or other non-standard dynamics. Unlike particle dark matter, their formation does not rely on new fundamental fields but on the amplification of primordial perturbations or exotic early-Universe processes. Depending on their mass, primordial black holes can evade Hawking evaporation and persist until today, contributing to or even constituting the dark matter abundance. They are searched for not through particle interactions but via astrophysical and cosmological signatures, such as gravitational lensing, distortions in the cosmic microwave background, or dynamical effects on stars and galaxies.

## References

- [1] Adapted from Danjon, A., "Le centenaire de la découverte de Neptune", Ciel et Terre, Vol. 62, p. 369 https://aetherczar.substack.com/p/523-the-search-for-vulcan#\_edn5
- [2] Wikipedia,
   https://commons.wikimedia.org/wiki/File:Perihelion\_
   precession.svg?uselang=en#Licensing
- [3] T. S. van Albada, J. N. Bahcall, K. Begeman and R. Sancisi, "The Distribution of Dark Matter in the Spiral Galaxy NGC-3198," Astrophys. J. **295** (1985), 305-313
- [4] Marc Türler, "The Milky Way's dark-matter halo reappears," CERN Courier, July 18, 2012. Available at: https://cerncourier.com/a/the-milky-ways-dark-matter-halo-reappears/.

- [5] NASA,
   https://www.spitzer.caltech.edu/image/
   ssc2011-05b-gravitational-lensing-in-action
- [6] A. E. Evrard, "Well of darkness," Nature, 394, pp.â€-122-123, 1998. https://www.nature.com/articles/BF28034.
- [7] NASA/CXC/M.Weiss, 1E 0657-56 animations, https://chandra.harvard.edu/photo/2006/1e0657/animations.html
- [8] S. Chabanier, M. Millea and N. Palanque-Delabrouille, "Matter power spectrum: from Ly $\alpha$  forest to CMB scales," Mon. Not. Roy. Astron. Soc. **489** (2019) no.2, 2247-2253 [arXiv:1905.08103 [astro-ph.CO]].
- [9] Wikipedia based on D. J. Eisenstein *et al.* [SDSS], "Detection of the Baryon Acoustic Peak in the Large-Scale Correlation Function of SDSS Luminous Red Galaxies," Astrophys. J. **633** (2005), 560-574 [arXiv:astro-ph/0501171 [astro-ph]]. https://commons.wikimedia.org/wiki/File:LSS\_theory.png
- [10] A. Silvestri and M. Trodden, "Approaches to Understanding Cosmic Acceleration," Rept. Prog. Phys. **72** (2009), 096901 [arXiv:0904.0024 [astro-ph.CO]].
- [11] Winther, H. A., "First lecture: Cosmology II (AST 5220 / AST 9420)," University of Oslo, Lecture Notes, 2025. https://www.uio.no/studier/emner/matnat/astro/AST5220/v25/dokumenter/lecture1\_2025.pdf
- [12] I. Tkachev, "Cosmology and Dark Matter," [arXiv:1802.02414 [gr-qc]].
- [13] D. Wands, O. F. Piattella and L. Casarini, "Physics of the Cosmic Microwave Background Radiation," Astrophys. Space Sci. Proc. **45** (2016), 3-39 [arXiv:1504.06335 [astro-ph.CO]].
- [14] M. Bauer and T. Plehn, "Yet Another Introduction to Dark Matter: The Particle Physics Approach," Lect. Notes Phys. **959** (2019), pp. Springer, 2019, [arXiv:1705.01987 [hep-ph]].
- [15] G. Gelmini and P. Gondolo, "DM Production Mechanisms," [arXiv:1009.3690 [astro-ph.CO]].
- [16] J. Billard, M. Boulay, S. Cebrián, L. Covi, G. Fiorillo, A. Green, J. Kopp, B. Majorovits, K. Palladino and F. Petricca, *et al.* "Direct detection of dark matter—APPEC committee report\*," Rept. Prog. Phys. **85** (2022) no.5, 056201 [arXiv:2104.07634 [hep-ex]].
- [17] M. Hütten and D. Kerszberg, "TeV Dark Matter Searches in the Extragalactic Gamma-ray Sky," Galaxies **10** (2022) no.5, 92 [arXiv:2208.00145 [astro-ph.HE]].
- [18] E. Hardy, "Higgs portal dark matter in non-standard cosmological histories," JHEP **06** (2018), 043 [arXiv:1804.06783 [hep-ph]].